




Cite this: *Chem. Commun.*, 2022, 58, 9758

Received 27th June 2022,
Accepted 4th August 2022

DOI: 10.1039/d2cc03561h

rsc.li/chemcomm

Structurally characterised intermediate of the oxidative addition of a heteroleptic germylene to gallanediyl†

Anna B cker,^a Christoph W lper,^a Gebhard Haberhauer^b and Stephan Schulz^b  ^{a,c}

Bond activation reactions using main group metal complexes are gaining increasing interest. We report on reactions of LGa (L = HC[C(Me)N(Ar)]₂, Ar = Dipp = 2,6-*i*-Pr₂C₆H₃) with heteroleptic tetraenes L'ECI (E = Ge, Sn; L' = N(SiMe₃)Ar), yielding the donor-acceptor complex LGa-Sn(Cl)L' (1) or the oxidative addition product L(Cl)GaGeL' (3). The reaction with DMPGeCl (DMP = 2,6-Mes₂C₆H₃, Mes = 2,4,6-Me₃C₆H₂) yielded LGa(μ-Cl)GeDMP (2), which represents an intermediate of the oxidative addition reaction. 1–3 were characterized by NMR and IR spectroscopy as well as by single crystal X-ray diffraction (sc-XRD), while their electronic nature was analyzed by quantum chemical calculations.

Oxidative addition and reductive elimination reactions are key steps in catalytic processes and typically call for transition metal complexes as they tend to easily change their electronic situation. Oxidative addition with rather nonpolar substrates such as H₂ and hydrocarbons mainly proceeds *via* a concerted mechanism with formation of a three-centered σ complex, whereas a bimolecular nucleophilic substitution is often observed with polar and electrophilic substrates, *i.e.* alkyl halides. The metal center undergoes nucleophilic attack at the less electronegative atom in the substrate, resulting in R–X bond cleavage and formation of a cationic [M–R]⁺ species, followed by rapid coordination of the anion. Low valent main group metal complexes, *i.e.* carbene-type group 13 (RM; M = Al, Ga, In) and group 14 compounds (R₂E; E = Si, Ge, Sn), with

energetically high lying HOMOs and low lying LUMOs show electronic similarities to transition metal complexes,¹ and were therefore successfully applied in bond activation and catalytic reactions.^{2–5} Oxidative addition is expected to proceed similar to transition metal complexes, *i.e.*, H₂ activation by cyclic and acyclic silylenes and germylenes followed a concerted mechanism,^{6a} whereas a singlet carbene reacted *via* a heterolytic mechanism.^{6b,c}

Oxidative addition of group 14 compounds to group 13 diyls LM has also been reported, including C–F bond activation by LAl^{7a,b} and a dinuclear gallanediyl,^{7c} as well as C–Cl bond activation by LGa.^{7d,e} Interestingly, indanediyl LIn reacted with alkyl iodides in a radical mechanism *via* homolytic bond cleavage.^{7f} Gallanediyl LGa on the other hand reacted with heavier tetravalent group 14 compounds, *i.e.*, SiCl₄, HSiCl₃, Me₂SnCl₂, Ph₃SnH, and Me₃PbCl,^{7d,8a,b} with oxidative addition. In contrast, reactions with divalent tetraenes EX₂ proceeded either with oxidative addition, *i.e.*, reactions with plumbylene Pb(OSO₂CF₃)₂^{8b} and silylene PhC(Nt-Bu)₂SiCl,^{9a} or with E–E bond formation as observed with Do–GeCl₂ (Do = IDipp = C[N(Dipp)CH]₂, Cy₃P) and SnCl₂,^{9b,c} respectively. Even though the reducibility of heavier tetraenes is expected to play a major role, the reaction mechanism and the reason behind different product formation could not be clearly identified.

We are generally interested in bond activation of group 13, 15, and 16 complexes with group 13 diyls LM,^{10–12} for which we have recently extended these studies to group 14 complexes. Si–X bond activation of SiBr₄ and IDippSiI₄ with LGa under CO atmosphere gave the first room temperature stable silylene carbonyl complexes [L(X)Ga]₂SiCO (X = Br, I),¹³ while heteroleptic metallasilylenes [L(Cl)MSi(Nt-Bu)₂]CPh were formed in reactions of LM (M = Al, Ga) with PhC(Nt-Bu)₂SiCl.^{9a} The carbonyl complexes serve as masked silylenes as shown in reactions with H₂ and NH₃, which occurred with oxidative addition and formation of the corresponding tetravalent silanes,¹³ whereas the heteroleptic metallasilylenes reacted with P₄ with unprecedented [2 + 1 + 1] fragmentation.^{9a,13}

^a Institute of Inorganic Chemistry, University of Duisburg-Essen, 45117 Essen, Germany. E-mail: stephan.schulz@uni-due.de

^b Institute of Organic Chemistry, University of Duisburg-Essen, 45117 Essen, Germany

^c Center for Nanointegration Duisburg-Essen (Cenide), University of Duisburg-Essen, 47057 Duisburg, Germany

† Electronic supplementary information (ESI) available: Experimental procedures, NMR and IR spectra, elemental analysis, crystallographic data and computational details. CCDC 2160059 (1), 2160060 (2), 2160061 (3), 2179253 (4), 2160062 (5), 2160063 (6), and 2160064 (7). For ESI and crystallographic data in CIF or other electronic format see DOI: <https://doi.org/10.1039/d2cc03561h>



Unfortunately, the isolation of the homoleptic metallasilylenes $[L(X)Ga]_2Si$ has failed, rendering mechanistic studies rather complicated, whereas the heteroleptic metallasilylenes reacted too fast. We therefore became interested in extending these studies to the heavier heteroleptic group 14 homologues, which were expected to be less reactive and therefore promising candidates for conducting mechanistic studies and evaluating the role of the central group 14 element.

Equimolar reactions of LGa^{14} with heteroleptic tetrylenes $L'ECl$ ($E = Ge, Sn^{15}$) either yielded the Lewis acid-base adduct $LGa-Sn(Cl)L'$ (**1**), or occurred with oxidative addition and formation of $L(Cl)GaGeL'$ (**3**). This is somewhat unanticipated since the heavier stannylene was expected to exhibit a lower reduction potential compared to the lighter germylene and since the Sn-Cl bond is slightly weaker than the Ge-Cl bond. However, the formation of **1** clearly shows that the reaction proceeds as a Lewis acid-base type reaction in which LGa serves as a Lewis base, thus supplying electron density into the empty p orbital of the stannylene. The same reaction mechanism is expected to occur with the germylene, but in this case, the adduct formation is followed by a Ge-Cl bond activation, resulting in the oxidative addition. This proposed mechanism is supported by the formation of $LGa(\mu-Cl)GeDMP$ (**2**), which was obtained by reacting LGa with $DMPGeCl$,¹⁶ especially since **2** represents an intermediate between adduct formation and oxidative addition (Scheme 1).

Compounds **1–3** were isolated in moderate yields (**1**: 43%, **2**: 43%, **3**: 48%) after re-crystallization from saturated solutions of toluene or *n*-hexane at $-20^\circ C$. The 1H and ^{13}C NMR spectra of **1–3** show resonances of the β -diketiminate (L) and the amine (**1**, **3**) or the DMP (**2**) ligands. *In situ* 1H -NMR studies proved that **1** and **2** are quantitatively formed immediately after dissolution of the starting reagents in toluene- d_8 at ambient temperature, while the *in situ* 1H NMR spectrum of **3** also shows the formation of small amounts of $LGaCl_2$ in benzene- d_6 . An isolated sample of **3** is stable in benzene solution at ambient temperature for one week, whereas **1** slowly decomposes within four days with formation of $LGaCl_2$ and L'_2Sn according to an *in situ* 1H NMR spectroscopy study (Fig. S25, ESI†). **2** rapidly decomposes within 90 minutes forming $LGaCl_2$ and unidentified products (Fig. S28, ESI†).

Single crystals were obtained from saturated solutions in toluene (**1**, **3**) and *n*-hexane (**2**) at $-20^\circ C$ as yellow (**1**) and purple (**3**) platelets or pale-yellow blocks (**2**). **1** crystallizes in the

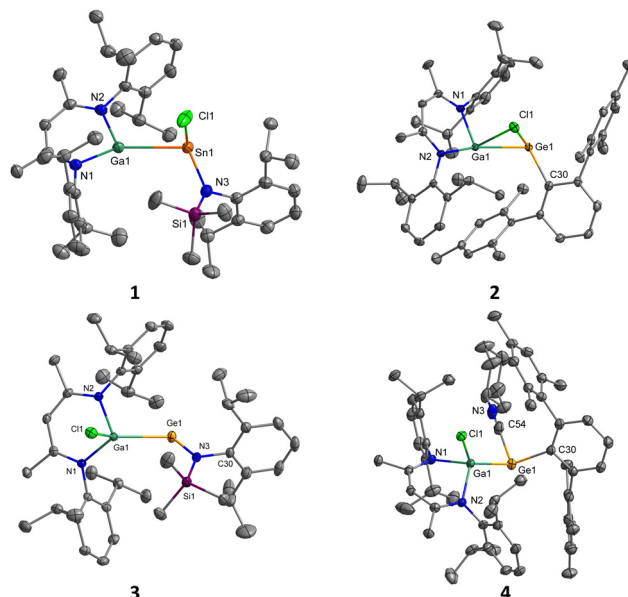
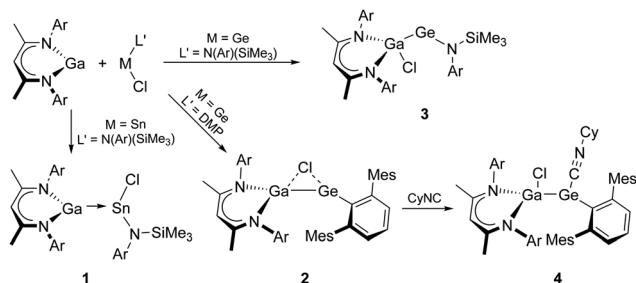


Fig. 1 Molecular structures of **1–4**. Displacement ellipsoids are set at 50% probability. Hydrogen atoms, alternate positions of the disordered parts and solvent molecules are omitted for clarity.

monoclinic space group $P2_1/c$, while **2** and **3** in the triclinic space group $P\bar{1}$ (Fig. 1), respectively. Selected bond lengths and angles are summarized in Table 1. The Sn-Cl moiety in **1** is disordered over two positions. The Ga-Sn bonds (2.8854(5) Å; 2.902(7) Å) are substantially elongated compared to those in $[K(tmeda)][R_2SnGa\{N(Ar)C(H)\}_2]$ ($R = CH(SiMe_3)_2$ 2.7186(6) Å; i -Pr $_3C_6H_5$ 2.6660(18) Å),¹⁷ $[L(Cl)Ga]_2SnMe_2$ (2.6236(7)–2.6328(7) Å)^{8a} and the metalloid tin clusters $[L(Cl)Ga]_2Sn_7$ (2.580(4)–2.598(3) Å) and $[L(Cl)Ga]_4Sn_{17}$ (2.5783(15)–2.5876(13) Å), respectively.^{9c} They are also longer than the calculated covalent single bond radii ($\sum r_{cov} = 2.64$ Å),¹⁸ but shorter than the sum of van der Waals radii ($\sum r_{vdw} = 4.04$ Å),¹⁹ thus indicating a rather weak donor-acceptor interaction. The Ga-Ge (2.5533(2) Å) and Ga-Cl bond length (2.2537(3) Å) in **3** are within the reported bond length ranges (Ga-Ge 2.390–2.592 Å; Ga-Cl 2.142–2.322 Å²⁰).

In remarkable contrast to **1** and **3**, **2** shows a triangular coordination of Ge-Ga with a μ^2 -bridging Cl atom that was only observed in transition metal complexes such as $LGa(\mu-Cl)-Rh(PPh_3)_2$.^{21,22} The Ga-Ge bond length of 2.4678(4) Å agrees with the sum of calculated covalent single bond radii ($\sum r_{cov} = 2.48$ Å),¹⁸ whereas both the Ge-Cl (2.4924(6) Å) and Ga-Cl



Scheme 1 Syntheses of compounds **1–4** ($Ar = Dipp$).

Table 1 Selected bond length [Å] and bond angles [$^\circ$] of **1–7**

	Ga-Cl	E-Cl	Ga-E	E-C/N	Ga-E-C/N
1	—	2.4917(14)	2.8854(5)	2.122(3)	112.07(9)
2	2.6076(6)	2.4924(6)	2.4678(4)	2.022(2)	113.38(6)
3	2.2537(3)	—	2.5533(2)	1.8424(11)	110.10(3)
4	2.2779(4)	—	2.4964(3)	2.0413(15)	116.79(4)
5	—	—	2.7894(4)	2.033(2)	106.50(7)
6	—	—	2.6217(4)	2.014(2)	108.23(6)
7	—	—	2.5985(4)	1.8162(15)	110.71(4)

E = Ge, compounds **2**, **3**, **4**, **6**, **7**; E = Sn, compounds **1**, **5**.



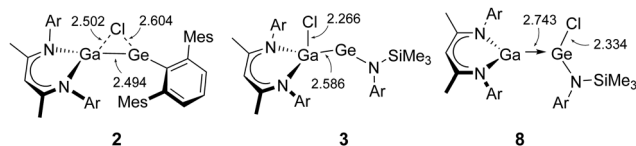


Fig. 2 Calculated (B3LYP-D3BJ/def2-TZVP) bond lengths [Å] of the germylene compounds **2**, **3** and **8** (Ar = Dipp).

bonds (2.6076(6) Å) are substantially elongated compared to those observed in DMPGeCl (2.120(2) Å),¹⁶ LGa(μ-Cl)Rh(PPh₃)₂ (2.485 Å),²² and L(Cl)Ga-substituted compounds (2.142–2.322 Å).²⁰ The R–E–Ga bond angles of **1–3** are very similar (**1** 112.07(9)°; **2** 113.38(6)°; **3** 110.10(3)°).

To gain a deeper understanding of the electronic nature and bonding situation of these complexes, we performed quantum chemical calculations on **1–3** and **8** (LGa–Ge(Cl)L'), which represents the germanium analogue of compound **1**, using B3LYP-D3BJ/def2-TZVP (Fig. 2).

The energy difference between **3** and **8** and thus for the oxidative addition of the Ge–Cl bond computes to 9.3 kcal mol^{−1} in favour of **3**. An analysis of the frontier orbitals of **1–3** and **8** shows (Fig. S37 and S38, ESI[†]) that the “empty” p orbital at Ge in **3** is stabilized by the electron lone pair of the adjacent nitrogen atom. In germylene **2**, the aryl system is unable to adequately stabilize the empty p orbital at Ge, which therefore requires the stabilizing effect of the bridging chlorine atom. QTAIM²³ calculations were performed for **2** (Fig. S43 and Tables S4, S5, ESI[†]). Further analysis reveals that the Laplacian of the electron density at the bond critical points in Ga–Cl and Ge–Cl bonds is positive, whereas the total energy densities (H_{CP}) are negative. This is consistent with a highly polarized covalent interaction.²⁴ The stabilizing effect of the bridging chlorine atom is further confirmed by calculations of reference compounds **S1–S6** (Fig. S39, ESI[†]). The smaller the electron-donating character of the substituent on the Ge atom, the shorter is the Ge–Cl distance and the larger is the Ga–Cl bond. It is also interesting to note that the Ga–Ge bond lengths decreases in the reference compounds **S1–S6** due to the stabilizing effect of the bridging chlorine atom. Accordingly, the Ga–Ge bond in **2** (2.494 Å) is also shorter than that in **3** (2.586 Å, Fig. 2). A comparison of the experimentally determined bond lengths with the calculated ones (Table 1 and Table S3, ESI[†]) shows that the highest deviations are found for the Ga–Cl (exp: 2.6076(6) Å; calc: 2.502 Å) and the Ge–Cl bonds (exp: 2.4924(6) Å; calc: 2.604 Å) in **2**. A reference calculation reveals that the energy changes upon modifying the Ga–Cl and Ge–Cl distances are very small in this structure (see Fig. S42, ESI[†]).

To support the description of **2** as an intermediate of the oxidative addition product, we studied its reactions with Lewis

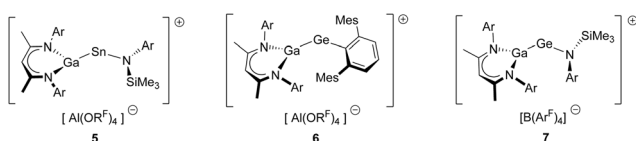


Fig. 3 Salts **5–7**.

bases (CyNC, IMe₄ (IMe₄ =: C[N(Me)CMe]₂)) and the strong Lewis acid B(C₆F₅)₃. The reaction of **2** with IMe₄ and B(C₆F₅)₃ proceeded with Ga–Ge bond cleavage and formation of IMe₄–Ge(Cl)DMP and LGa, as well as LGa–B(C₆F₅)₃²⁵ and DMPGeCl as was confirmed by *in situ* ¹H NMR spectroscopy studies (Fig. S33–S35, ESI[†]). In remarkable contrast, the reaction with isonitrile CyNC gave the CyNC-coordinated germylene L(Cl)GaGe–(CNCy)DMP **4** (Scheme 1 and Fig. S36, ESI[†]). Single crystals of **4** were obtained after storing an *n*-hexane solution at ambient temperature. The Ga–Ge (2.4964(3) Å) and Ge–C_{DMP} 2.0413(15) Å bond lengths as well as the Ga–Ge–C_{DMP} bond angle (116.79(4)°) of **4** are very similar to those of **2** (Table 1). Despite its dative character, the Ge–C_{CyNC} bond in **4** (2.0037(18) Å) is slightly shorter than the Ge–C_{DMP} bond (2.0413(15) Å).

To further investigate the stabilizing role of the chlorine substituent in **1–3**, we studied halide abstraction reactions with Li(Al(OR^F)₄) (R^F = C(CF₃)₃) and Na(B(Ar^F)₄) (Ar^F = 3,5-(CF₃)₂C₆H₃), respectively, yielding the corresponding salts **5–7** in low to moderate yields (**5** 11%, **6** 39%, **7** 25%) (Fig. 3).

Compounds **5–7** are stable in solutions in fluorobenzene and 1,2-difluorobenzene. Due to the insolubility or instability of the compounds in C₆D₆, C₆D₅Br, CD₂Cl₂ and THF-*d*₈, the NMR spectra were recorded in a mixture of benzene-*d*₆ with fluorobenzene (**6**) or toluene-*d*₈ with 1,2-difluorobenzene (**5**, **7**), respectively. The ¹H and ¹³C NMR spectra of **5–7** feature the signals of the β-diketiminato (L) and the amide (**5**, **7**) or the DMP ligand (**6**). ¹H NMR resonances of the γ-CH and CH₃ groups (L) of **5** are low-field shifted compared to **1**, whereas resonances of the *i*-Pr and Me₃Si groups are high-field shifted. Comparable trends are observed for compound **7** with respect to compound **3** and were also reported for L(X)Ga-substituted group 15 cations.²⁶

Single crystals of **5–7** were isolated as orange blocks from fluorobenzene solutions layered with *n*-hexane upon storage at ambient temperature. **5** and **6** crystallize in the monoclinic space group *P*2₁/*c* and **7** in the triclinic space group *P*1̄, respectively (Fig. 4). Selected bond lengths and bond angles are summarized in Table 1.

The Ga–Sn (2.7894(5) Å) and the Sn–N (2.033(2) Å) bonds in **5** are shorter than those of **1** (Ga–Sn 2.8854(5) Å; Sn–N 2.122(3) Å) as is expected due to the positive charge at the Sn center, which results in an enhanced Lewis acidity of the Sn atom. In contrast, the Ga–Ge (2.5985(4) Å) and Ge–N (1.8162(15) Å) bond lengths in **7** are almost comparable to those in the neutral

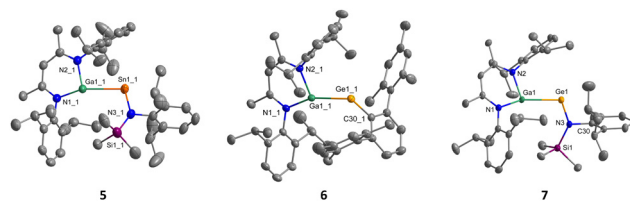


Fig. 4 Molecular structures of the cations in **5–7**. Displacement ellipsoids are set at 50% probability. Hydrogen atoms, alternate positions of the disordered parts, counter anions and solvent molecules are omitted for clarity.



compound **3** (Ga–Ge 2.5533(2) Å; Ge–N 1.8424(11) Å). Surprisingly, the Ga–Ge bond in **6** (2.6217(4) Å) is significantly longer whereas the Ge–C bond length (2.014(2) Å) is slightly shorter than those in the neutral complex **2** (Ga–Ge 2.4678(4) Å; Ge–C 2.022(2) Å). The Ga–Ge–N bond angle in **7** (110.71(4)°) remains constant after the chloride abstraction from **3** (110.10(3)°), whereas the Ga–E–R bond angles in **5** (106.50(7)°) and **6** (108.23(6)°) are smaller than those in **1** (112.07(9)°) and **2** (113.38(6)°).

To interpret these results, the cations in **5**–**7** were studied by quantum chemical calculations. In all of the studied cations, the LUMO consists of a binding linear combination of the empty p orbitals at the Ga and E centers (Fig. S40, ESI†), hence the positive charge is distributed over both centers. The experimentally observed changes in the Ga–E bond lengths due to halide abstraction are also found in the calculations of **1**–**3** and **5**–**7**. The elongation of the Ga–Ge bond at the transition from neutral compound **2** to the cation **6** can be mainly attributed to the removal of the stabilizing chlorine bridge, which becomes obvious when looking at the reference compounds **S3**, **S7** and **S8** (Fig. S41, ESI†). In compound **S7**, the Cl atom on the Ga center is replaced by a methyl group, which therefore cannot form an electronically stabilizing bridge. As a result, the Ga–Ge bond length in **S7** (2.547 Å) is significantly elongated compared to that in **S3** (2.502 Å) by roughly 45 pm. The abstraction of the (anionic) CH₃ ligand in **S7** leads to only a small increase (+0.05 Å) of the Ga–Ge distance, roughly half of the increase observed for the removal of the Cl anion in compound **2** (+0.10 Å).

To conclude, LGa reacted with Ar(SiMe₃)NECl following either an adduct formation (E = Sn, **1**) or an oxidative addition (E = Ge, **3**), whereas the reaction with DMPGeCl gave compound **2**, which represents an isolable intermediate of the oxidative addition reaction. Quantum chemical calculations provided deeper insights into the role of electron donating groups attached to the germanium atom, which play a crucial role in its electronic stabilization. In compound **3**, the empty p orbital is stabilized by the electron lone pair of the amino ligand, whereas in the case of **2**, the bridging Cl atom is necessary since the DMP aryl system is unable to adequately stabilize the empty p orbital at the Ge centre. Our studies clearly revealed the crucial electronic role of the tetraphenyl ligand L' on the product formation. Finally, the effect of Cl abstraction on the structures of the cations in salts **5**–**7** was also demonstrated.

Financial support by the DFG (SCHU1069/26-1) and the University of Duisburg-Essen is acknowledged.

Conflicts of interest

There are no conflicts to declare.

Notes and references

- (a) P. P. Power, *Nature*, 2010, **463**, 171; (b) R. L. Melen, *Chem. Soc. Rev.*, 2016, **45**, 775; (c) L. C. Wilkins and R. L. Melen, *Coord. Chem. Rev.*, 2016, **324**, 123; (d) C. Weetman and S. Inoue, *Chem. Cat. Chem.*, 2018, **10**, 4213; (e) R. L. Melen, *Science*, 2019, **363**, 479.
- M. Asay, C. Jones and M. Driess, *Chem. Rev.*, 2011, **111**, 354.
- (a) T. Chu and G. I. Nikonov, *Chem. Rev.*, 2018, **118**(7), 3608; (b) Y. Liu, J. Li, X. Ma, Z. Yang and H. W. Roesky, *Coord. Chem. Rev.*, 2018, **374**, 387; (c) M. Zhong, S. Sinhababu and H. W. Roesky, *Dalton Trans.*, 2020, **49**, 1351.
- C. Shan, S. Yao and M. Driess, *Chem. Soc. Rev.*, 2020, **49**, 6733.
- (a) S. Yadav, S. Saha and S. S. Sen, *ChemCatChem*, 2016, **8**, 468; (b) T. J. Hadlington, M. Driess and C. Jones, *Chem. Soc. Rev.*, 2018, **47**, 4176.
- (a) Y. Wang and J. Ma, *J. Organomet. Chem.*, 2009, **694**, 2567; (b) G. D. Frey, V. Lavallo, B. Donnadieu, W. W. Schöller and G. Bertrand, *Science*, 2007, **316**, 439; (c) D. Devarajan, C. E. Doubleday and D. H. Ess, *Inorg. Chem.*, 2013, **52**, 8820.
- (a) M. R. Crimmin, M. J. Butler and A. J. P. White, *Chem. Commun.*, 2015, **51**, 15994; (b) T. Chu, Y. Boyko, I. Korobkov and G. I. Nikonov, *Organometallics*, 2015, **34**, 5363; (c) O. Kysliak, H. Görls and R. Kretschmer, *J. Am. Chem. Soc.*, 2021, **143**, 142; (d) A. Kempter, C. Gemel and R. A. Fischer, *Inorg. Chem.*, 2008, **47**, 7279; (e) C. Helling, C. Ganesamoorthy, C. Wölper and S. Schulz, *Dalton Trans.*, 2022, **51**, 2050; (f) M. S. Hill, P. B. Hitchcock and R. Pongtavornpinyo, *Inorg. Chem.*, 2007, **46**, 3783.
- (a) A. Seifert, D. Scheid, G. Linti and T. Zessin, *Chem. – Eur. J.*, 2009, **15**, 12114; (b) G. Prabusankar, C. Gemel, M. Winter, R. W. Seidel and R. A. Fischer, *Chem. – Eur. J.*, 2010, **16**, 6041.
- (a) J. Schoening, A. Gehlhaar, C. Wölper and S. Schulz, *Chem. – Eur. J.*, 2022, **28**, e202201031; (b) A. Doddi, C. Gemel, M. Winter, R. A. Fischer, C. Goedecke, H. S. Rzepa and G. Frenking, *Angew. Chem., Int. Ed.*, 2013, **52**, 450; (c) G. Prabusankar, A. Kempter, C. Gemel, M. K. Schröter and R. A. Fischer, *Angew. Chem., Int. Ed.*, 2008, **47**, 7234.
- C. Ganesamoorthy, D. Bläser, C. Wölper and S. Schulz, *Organometallics*, 2015, **34**, 2991.
- (a) L. Tüscher, C. Ganesamoorthy, D. Bläser, C. Wölper and S. Schulz, *Angew. Chem., Int. Ed.*, 2015, **54**, 10657; (b) J. Krüger, C. Ganesamoorthy, L. John, C. Wölper and S. Schulz, *Chem. – Eur. J.*, 2018, **24**, 9157; (c) C. Helling, C. Wölper and S. Schulz, *J. Am. Chem. Soc.*, 2018, **140**, 5053; (d) M. K. Sharma, C. Wölper, G. Haberhauer and S. Schulz, *Angew. Chem., Int. Ed.*, 2021, **60**, 6784; (e) C. Ganesamoorthy, C. Helling, C. Wölper, W. Frank, E. Bill, G. E. Cutsail III and S. Schulz, *Nat. Commun.*, 2018, **9**, 87; (f) C. Helling, G. E. Cutsail III, H. Weinert, C. Wölper and S. Schulz, *Angew. Chem., Int. Ed.*, 2020, **59**, 7561; (g) H. M. Weinert, C. Wölper, J. Haak, G. E. Cutsail III and S. Schulz, *Chem. Sci.*, 2021, **12**, 14024.
- S. Schulz, C. Ganesamoorthy, G. Bendt, D. Bläser and C. Wölper, *Dalton Trans.*, 2015, **44**, 5153.
- (a) C. Ganesamoorthy, J. Schoening, C. Wölper, L. Song, P. R. Schreiner and S. Schulz, *Nat. Chem.*, 2020, **12**, 608; (b) J. Schoening, C. Ganesamoorthy, C. Wölper, E. Solel, P. R. Schreiner and S. Schulz, *Dalton Trans.*, 2022, **51**, 8249.
- N. J. Hardman, B. E. Eichler and P. P. Power, *Chem. Commun.*, 2000, 1991.
- M. Brynda, R. Herber, P. B. Hitchcock, M. F. Lappert, I. Nowik, P. P. Power, A. V. Protchenko, A. Růžicka and J. Steiner, *Angew. Chem., Int. Ed.*, 2006, **45**, 4333.
- R. S. Simons, L. Pu, M. M. Olmstead and P. P. Power, *Organometallics*, 1997, **16**, 1920.
- S. P. Green, C. Jones, K. A. Lippert, D. P. Mills and A. Stasch, *Inorg. Chem.*, 2006, **45**, 7242.
- P. Pyykkö and M. Atsumi, *Chem. – Eur. J.*, 2009, **15**, 186.
- M. Mantina, A. C. Chamberlin, R. Valero, C. J. Cramer and D. G. Truhlar, *J. Phys. Chem. A*, 2009, **113**(19), 5806.
- Search for Ga–Ge bonds in CSD 5.43 gave 15 hits (2.390–2.592 Å, mean 2.47(5) Å). Search for L(Cl)Ga fragment gave 79 hits (2.142–2.322 Å, mean 2.23(3) Å). C. R. Groom, I. J. Bruno, M. P. Lightfoot and S. C. Ward, *Acta Crystallogr., Sect. B: Struct. Sci., Cryst. Eng. Mater.*, 2016, **72**, 171–179.
- U. Chakraborty, B. Mühldorf, N. J. C. van Velzen, B. de Bruin, S. Harder and R. Wolf, *Inorg. Chem.*, 2016, **55**, 3075.
- A. Kempter, C. Gemel, N. J. Hardman and R. A. Fischer, *Inorg. Chem.*, 2006, **45**, 3133.
- R. F. W. Bader, *Atoms in Molecules: A Quantum Theory*, Oxford University Press, Oxford, UK, 1990.
- E. Espinosa, I. Alkorta, J. Elguero and E. Molins, *J. Chem. Phys.*, 2002, **117**, 5529.
- N. J. Hardman, P. P. Power, J. D. Gorden, C. L. B. Macdonald and A. H. Cowley, *Chem. Commun.*, 2001, 1866.
- (a) B. Li, C. Wölper, G. Haberhauer and S. Schulz, *Angew. Chem., Int. Ed.*, 2021, **60**, 1986; (b) J. Krüger, C. Wölper, G. Haberhauer and S. Schulz, *Inorg. Chem.*, 2022, **61**, 597.

